AEDC-TR-75-158

MOTION ANALYSIS PROCEDURE FOR ASYMMETRIC VEHICLES

VON KÁRMÁN GAS DYNAMICS FACILITY
ARNOLD ENGINEERING DEVELOPMENT CENTER
AIR FORCE SYSTEMS COMMAND
ARNOLD AIR FORCE STATION, TENNESSEE 37389

May 1976

Final Report for Period July 1973 — June 1975

Prepared for

DIRECTORATE OF TECHNOLOGY (DY)
ARNOLD ENGINEERING DEVELOPMENT CENTER
ARNOLD AIR FORCE STATION, TENNESSEE 37389

NOTICES

When U. S. Government drawings specifications, or other data are used for any purpose other than a definitely related Government procurement operation, the Government thereby incurs no responsibility nor any obligation whatsoever, and the fact that the Government may have formulated, furnished, or in any way supplied the said drawings, specifications, or other data, is not to be regarded by implication or otherwise, or in any manner licensing the holder or any other person or corporation, or conveying any rights or permission to manufacture, use, or sell any patented invention that may in any way be related thereto.

Qualified users may obtain copies of this report from the Defense Documentation Center.

References to named commercial products in this report are not to be considered in any sense as an endorsement of the product by the United States Air Force or the Government.

This report has been reviewed by the Information Office (OI) and is releasable to the National Technical Information Service (NTIS). At NTIS, it will be available to the general public, including foreign nations.

APPROVAL STATEMENT

This technical report has been reviewed and is approved for publication.

FOR THE COMMANDER

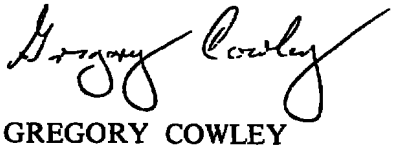

GREGORY COWLEY
Second Lieutenant, USAF
Research and Development
Division
Directorate of Technology

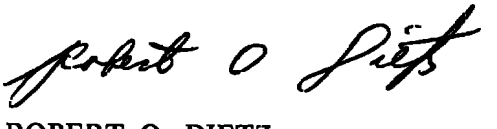

ROBERT O. DIETZ
Director of Technology

REPORT DOCUMENTATION PAGE	READ INSTRUCTIONS BEFORE COMPLETING FORM
1 REPORT NUMBER AEDC-TR-75-158	2 GOVT ACCESSION NO. / 3 RECIPIENT'S CATALOG NUMBER
4. TITLE (and Subtitle) MOTION ANALYSIS PROCEDURE FOR ASYMMETRIC VEHICLES	5 TYPE OF REPORT & PERIOD COVERED Final Report - July 1973 - June 1975 6 PERFORMING ORG. REPORT NUMBER
7 AUTHOR(s) C. J. Welsh and W. R. Lawrence - ARO, Inc.	8 CONTRACT OR GRANT NUMBER(s)
9 PERFORMING ORGANIZATION NAME AND ADDRESS Arnold Engineering Development Center (DY) Air Force Systems Command Arnold Air Force Station, Tennessee 37389	10. PROGRAM ELEMENT, PROJECT, TASK AREA & WORK UNIT NUMBERS Program Element 65807F
11 CONTROLLING OFFICE NAME AND ADDRESS Arnold Engineering Development Center (DYFS) Air Force Systems Command Arnold Air Force Station, Tennessee 37389	12. REPORT DATE May 1976 13 NUMBER OF PAGES 27
14 MONITORING AGENCY NAME & ADDRESS(if different from Controlling Office)	15. SECURITY CLASS. (of this report) UNCLASSIFIED 15a. DECLASSIFICATION/DOWNGRADING SCHEDULE N/A

16 DISTRIBUTION STATEMENT (of this Report)

Approved for public release; distribution unlimited.

17 DISTRIBUTION STATEMENT (of the abstract entered in Block 20, if different from Report)

18 SUPPLEMENTARY NOTES

Available in DDC

19 KEY WORDS (Continue on reverse side if necessary and identify by block number)

facility development
free field motion
aerodynamic conditions
aerodynamic drag coefficients
aeroballistics ranges
elliptic forms
asymmetry

20 ABSTRACT (Continue on reverse side if necessary and identify by block number)

The report discusses a recently developed procedure for analysis of free-flight motion to determine the aerodynamic coefficients of a vehicle having appreciable aerodynamic and inertia asymmetries. Aerodynamic data obtained by using this procedure in aeroballistic range tests of elliptic cross-section bodies indicate the potential usefulness of the developed procedure.

DD FORM 1 JAN 73 1473 EDITION OF 1 NOV 65 IS OBSOLETE

PREFACE

The work reported herein was conducted by the Arnold Engineering Development Center (AEDC), Air Force Systems Command (AFSC), under Program Element 65807F. The results were obtained by ARO, Inc. (a subsidiary of Sverdrup & Parcel and Associates, Inc.), contract operator of the AEDC, AFSC, Arnold Air Force Station, Tennessee. The work was done under ARO Project Nos. VF421-12GA and V32S-39A. The authors of this report were C. J. Welsh and W. R. Lawrence, ARO, Inc. The manuscript (ARO Control No. ARO-VKF-TR-75-83) was submitted for publication on June 19, 1975.

CONTENTS

ILLUSTRATIONS

TABLE

1.0 INTRODUCTION

Initial reentry and space vehicles of primary interest were, in general, axisymmetric. A capability for free-flight testing of such configurations having force and moment characteristics linear with angle of attack has existed for some time, both in wind tunnels and in aeroballistic ranges, for example, Refs. 1 and 2. With the imposed restraint of linear force and moment characteristics, closed form solution of the differential equations of motion could be obtained and fitted to the measured motion histories experienced by the bodies. In such a fitting procedure, a fit of the measured motion history is obtained by adjusting the unknown parameters in the motion equations. More recently the development of numerical-integration fitting procedures (see Refs. 3 and 4), in which the differential equations of motion are used directly in fitting the measured motion histories, has permitted handling axisymmetric configurations having nonlinear aerodynamic coefficients. However, many of the current and proposed vehicles of interest have appreciable asymmetries. Motion histories of such vehicles, in general, cannot be described adequately with the standard motion equations that have been used satisfactorily with axisymmetric bodies. Hence, asymmetric vehicles have represented an area in which the testing capability was inadequate. It should be noted that asymmetries as used here refer to inertia asymmetries and to primary aerodynamic asymmetries which involve significant differences between C_{N_α} and C_{N_β} and between $|C_{m_\alpha}|$ and $|C_{n_\beta}|$. This is in contrast to publications in which asymmetries refer to aerodynamic trim terms.

This report presents a discussion of the development of a procedure (numerical-integration fitting approach in conjunction with revised motion equations) compatible with bodies having appreciable aerodynamic and inertia asymmetries. Further, free-flight experimental data for elliptic cross-section bodies are presented. The experiments were conducted in the von Kármán Gas Dynamics Facility (VKF), AEDC, 1000-ft Hyperballistic Range G.

2.0 MOTION EQUATIONS FOR ASYMMETRIC BODIES

The conventional motion fitting technique as used for many years is restricted to axisymmetric bodies and, as noted previously, is restricted to bodies having linear force and moment characteristics (see Ref. 5). The closed form solution of the yawing-motion differential equations associated with that technique is also dependent on the ratio of

the rolling velocity of the body to its longitudinal velocity being constant. Another area of concern in that fitting technique is the axis systems involved. Although the experimental yawing motion of a body (measured with a range shadowgraph system) is defined relative to a fixed-plane axis system, the yawing-motion equation used is referenced to a nonrolling axis system so that the equation can be written in closed form. A sketch of the fixed-plane axis system is shown in Fig. 1a. In this system $\phi = 0$ and, by definition, the y-axis of the fixed-plane axis system remains in the $(x_o\text{-}y_o)$ plane. In the nonrolling axis system, the rolling velocity (p) is zero by definition. This restraint corresponds to $\dot{\phi} = \dot{\psi} \sin \theta$; however, for small amplitudes, the two axis systems are comparable. Although errors resulting from the two-axis systems approach are believed to be negligibly small, in general, their use is an undesirable characteristic of the fitting technique as is the velocity ratio restraint.

The numerical integration fitting technique (NIF technique) developed for axisymmetric bodies (see Refs. 3 and 4) is significant in that it permits removing some of the undesirable features of the conventional aeroballistic range technique. In the NIF technique for axisymmetric bodies, the differential motion equations are referenced to a fixed-plane axis system, the velocity ratio restraint is removed, and nonlinear aerodynamic force and moment characteristics can be handled. An additional feature of this technique is that the motion histories of more than one flight can be fit simultaneously. This multi-fit feature extends the capability of defining nonlinearities by permitting the use of flights of the same configuration but which experienced different mean amplitude levels. However, a fundamental and undesirable feature still is involved with the NIF technique for axisymmetric bodies -- appreciable aerodynamic or inertia asymmetries can not be handled.

The present study has been directed toward extending the capability of the NIF technique such that free-flight motion histories of bodies with appreciable asymmetries can be analyzed adequately. Definition of the motion equations for asymmetric bodies follows the same approach employed with axisymmetric bodies in which the basic relations of Newton are used:

$$\dot{L} = F$$

and

$$\dot{H} = M$$

Here, L and H are the linear and angular momentum of the body and F and M are the corresponding force and moment.

The problem of defining the motion equations is simplified for asymmetric bodies by using a fixed-body axis system (rolling axis system), rather than the fixed-plane axis system, in conjunction with an earth-fixed axis system (see Fig. 1b). The time rate of changes of the linear and angular momentum for the general constant mass body can be written (see, for example, Ref. 6):

$$\dot{L}_x = (\dot{u} + qw - rv)m \tag{1}$$

$$\dot{L}_y = (\dot{v} + ru - pw)m \tag{2}$$

$$\dot{L}_z = (\dot{w} + pv - qu)m \tag{3}$$

$$\dot{H}_x = I_x\dot{p} - I_{xy}\dot{q} - I_{xz}\dot{r} + qr(I_z - I_y) - pqI_{xz} - q^2 I_{yz} + r^2 I_{yz} + rpI_{xy} \tag{4}$$

$$\dot{H}_y = I_y\dot{q} - I_{xy}\dot{p} - I_{yz}\dot{r} + pr(I_x - I_z) - rqI_{xy} - r^2 I_{xz} + p^2 I_{xz} + pqI_{yz} \tag{5}$$

$$\dot{H}_z = I_z\dot{r} - I_{xz}\dot{p} - I_{yz}\dot{q} + pq(I_y - I_x) - p^2 I_{xy} - prI_{yz} + q^2 I_{xy} + qrI_{xz} \tag{6}$$

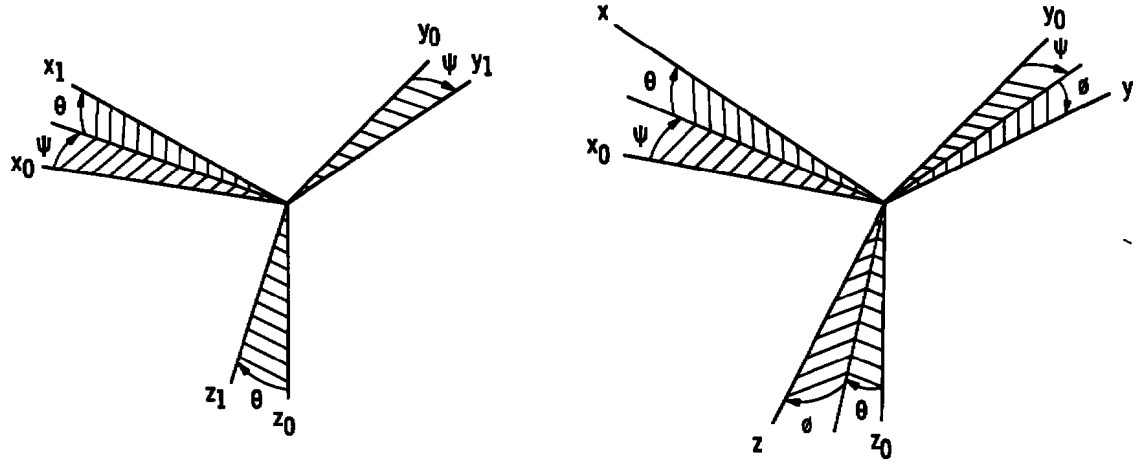

a. (x_1, y_1, z_1) Fixed-plane axis system, (x_0, y_0, z_0) Earth-fixed axis system

b. (x, y, z) Fixed-body axis system, (x_0, y_0, z_0) Earth-fixed axis system

Figure 1. Axis systems.

As all current and proposed reentry type missiles have at least one plane of symmetry, the angular momentum equations are simplified by restricting the equations to bodies for which the (x-z) plane is a plane of symmetry.

Hence,

$$\dot{H}_x = I_x\dot{p} - I_{xz}\dot{r} + qr(I_z - I_y) - pqI_{xz} \tag{7}$$

$$\dot{H}_y = I_y\dot{q} - pr(I_z - I_x) + I_{xz}(p^2 - r^2) \tag{8}$$

$$\dot{H}_z = I_z\dot{r} + pq(I_y - I_x) + I_{xz}(qr - \dot{p}) \tag{9}$$

Note that only one cross product of inertia component (I_{xz}) is involved for bodies for which the (x-z) plane is a plane of symmetry.

Although the inertia terms associated with an asymmetric body are easily defined, the components of the aerodynamic forces and moments along the three axes of the body-fixed axis system can be very difficult to define.

In Sketch 1 below, the angle (σ) defines the orientation of the plane of the total yaw angle (δ) relative to the body-fixed axis system.* In contrast to the usual derivations of motion equations for asymmetric bodies (see, for example, Ref. 6), it is apparent that the general yawing motion of an asymmetric body can involve in-plane and out-of-plane forces and moments that are functions of σ. Of the forces and moments

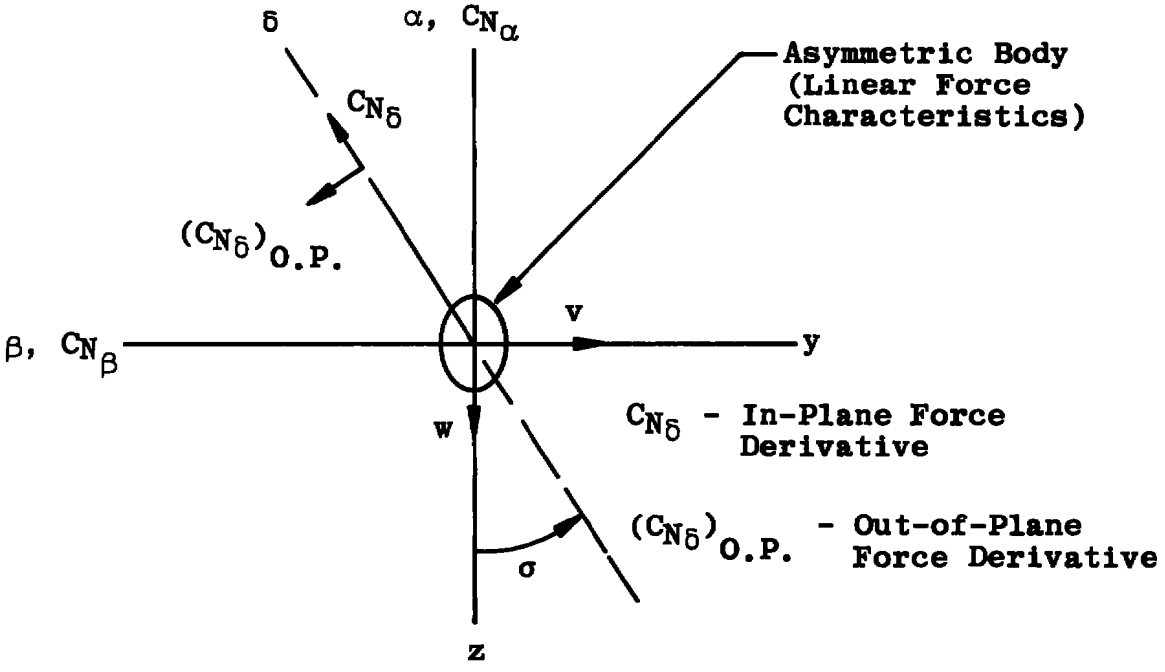

Sketch 1

that are dependent on the roll orientation of the total yaw plane, it is believed that the following ones are of primary concern:

1. The in-plane and out-of-plane static forces and their corresponding static moments and
2. The increment involved in the static roll moment.

The additional aerodynamic terms corresponding to the above forces and moments are the ones that are examined here. The problem of defining the aerodynamic terms for an asymmetric body can be better appreciated by first examining the forces on the axisymmetric body in Sketch 2 below:

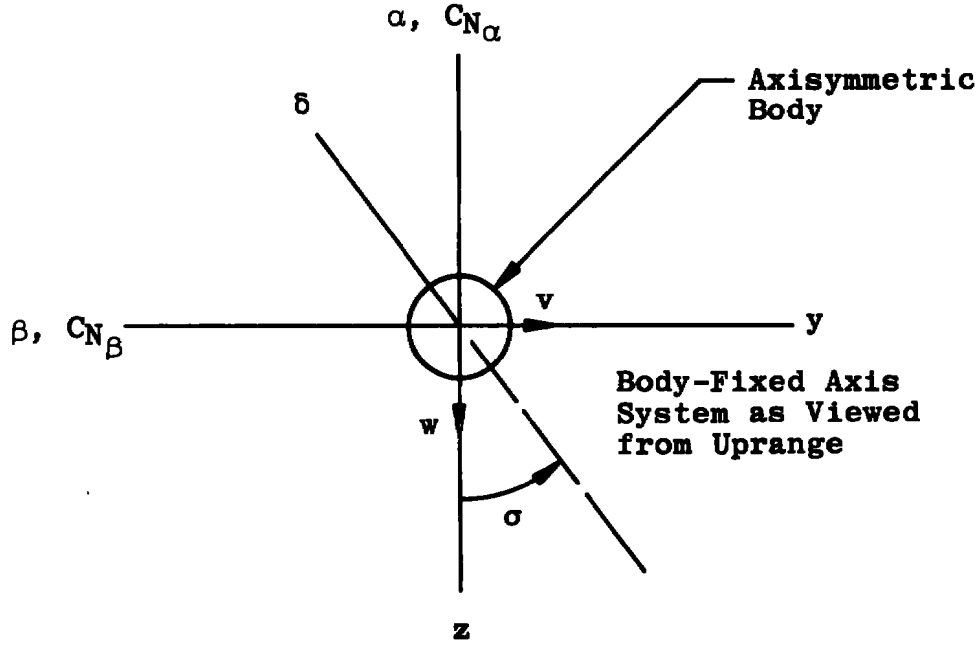

Sketch 2

Again, δ is the total yaw angle and σ is the orientation angle of the total yaw plane relative to the y and z axes. From aerodynamic symmetry considerations, there will be no out-of-plane force involved, and the normal force coefficient in the δ-direction can be written for a body having a cubic force variation,

$$(C_N)_{\delta\text{-DIR}} = C_{N_\delta} \sin\delta + C_{N_{3\delta}} (\sin\delta)^3$$

where

$$\sin\delta = \frac{\sqrt{w^2 + v^2}}{V}$$

and

$$C_{N_\delta} = \left[\frac{\partial C_N}{\partial (\sin \delta)}\right]_{\sin \delta \to 0}$$

Hence,

$$(C_N)_{\delta\text{-DIR}} = C_{N_\delta} \frac{\sqrt{w^2 + v^2}}{V} + C_{N_{3\delta}} \left(\frac{\sqrt{w^2 + v^2}}{V}\right)^3$$

and the component in the α-direction is

$$C_{N_z} = \left[C_{N_\delta} \frac{\sqrt{w^2 + v^2}}{V} + C_{N_{3\delta}} \left(\frac{\sqrt{w^2 + v^2}}{V}\right)^3\right] \cos \sigma$$

where

$$\cos \sigma = \frac{w}{\sqrt{w^2 + v^2}}$$

Hence

$$C_{N_z} = C_{N_\delta} \left(\frac{w}{V}\right) + C_{N_{3\delta}} \left(\frac{w^2 + v^2}{V^3}\right) w$$

$$= C_{N_\delta} \left(\frac{w}{V}\right) + C_{N_{3\delta}} \left(\frac{w}{V}\right)^3 + C_{N_{3\delta}} \left(\frac{v^2 w}{V^3}\right)$$

$$= C_{N_\alpha} \left(\frac{w}{V}\right) + C_{N_{3\alpha}} \left(\frac{w}{V}\right)^3 + C_{N_{3\alpha}} \left(\frac{v^2 w}{V^3}\right)$$

Replacing C_{N_δ} and $C_{N_{3\delta}}$ with C_{N_α} and $C_{N_{3\alpha}}$, respectively, in the last expression follows from the force derivative of an axisymmetric body being independent of σ. The force coefficient in the β-direction can be written similarly. The point of interest that can be observed in the above expressions is that the normal force, in the δ-direction, for an axisymmetric body having a linear or nonlinear force coefficient is a function of only δ. Similarly, in the case of the linear portion of the force coefficient, a component, say in the α-direction, is dependent only on the α-motion. However, the α-component of the nonlinear portion of the force coefficient is dependent on both the α-motion and the β-motion

experienced by the body. Similar comments obviously hold for components in the β-direction. It is important to recognize that the total normal force for an axisymmetric body being independent of σ permits one to easily define expressions for the required components in the α- and β-directions.

In the case of an asymmetric body having a linear force variation (see Sketch 1), C_{N_α} and C_{N_β} are the corresponding force derivatives if all of the yawing motion is either in the α- or β-planes, respectively. As C_{N_β} can be different from C_{N_α}, it follows that C_{N_δ}, normal force derivative in the plane of the total yaw angle (δ), will necessarily vary with σ, the orientation angle of the plane of the total yaw angle. Further, the out-of-plane force derivative $[(C_{N_\delta})_{O.P.}]$ will also be a function of σ. It follows that the variations of C_{N_δ} and $(C_{N_\delta})_{O.P.}$ with σ are required; however, there is a very limited amount of experimental data available to aid in defining precisely the variation of either C_{N_δ} or $(C_{N_\delta})_{O.P.}$. Hence, approximate variations for both C_{N_δ} and $(C_{N_\delta})_{O.P.}$ with σ have been deduced. These are given below and are believed to be quite adequate for bodies for which the force derivatives don't change appreciably between positive and negative yaw angles.

It is important to note that, in the defined variation for C_{N_δ}, two basic parts are involved. One part is dependent on the roll orientation (σ); whereas the other part is independent of σ. The approximate variation for C_{N_δ} used is

$$C_{N_\delta} = \left(C_{N_\delta}\right)_{mean} + \Delta C_{N_\delta}$$

Here, $(C_{N_\delta})_{mean}$ is the portion of C_{N_δ} that is independent of σ. Observe that the direction of ΔC_{N_δ} is indicated in Sketch 3. Also shown in Sketch 3 is ΔC_{N_β}, which is defined here to be the difference between C_{N_α} and C_{N_β}

$$\Delta C_{N_\beta} = C_{N_\beta} - C_{N_\alpha}$$

Note that $(C_{N_\delta})_{mean}$ corresponds to C_{N_α} in the ΔC_{N_β} expression, and that ΔC_{N_δ} (dependent on σ) is a function of ΔC_{N_β} and can be written

$$\Delta C_{N_\delta} = \Delta C_{N_\beta} |\sin \sigma| = \Delta C_{N_\beta} \times \frac{|v|}{\sqrt{w^2 + v^2}}$$

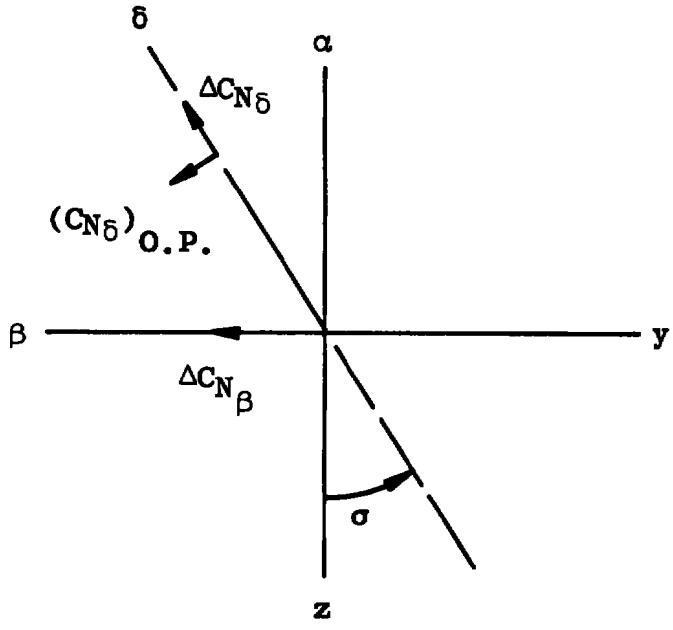

Sketch 3

This variation for ΔC_{N_δ} follows from the boundary conditions (see Sketch 3), $\Delta C_{N_\delta} = 0$ at $\sigma = 0$ and $\Delta C_{N_\delta} = \Delta C_{N_\beta}$ at $\sigma = 90°$. The expression for C_{N_δ} can now be written:

$$C_{N_\delta} = C_{N_\alpha} + \Delta C_{N_\beta} \frac{|v|}{\sqrt{w^2 + v^2}} \tag{10}$$

Further, the assumed variation of $(C_{N_\delta})_{O.P.}$ (see Sketch 3) with σ is

$$C_{N_\delta\ O.P.} = K_1 |\sin 2\sigma| = 2K_1 \frac{|wv|}{\sqrt{w^2 + v^2}} \tag{11}$$

This variation follows from the boundary conditions $[(C_{N_\delta})_{O.P.} = 0]$ for $\sigma = 0$ and 90 deg and has a maximum value at $\sigma = 45$ deg. Note that $K_1 = (C_{N_\delta})_{O.P.}$ at $\sigma = 45$ deg.

The resulting normal force expressions derived here for asymmetric bodies are listed below and are consistent with the following restraints. The portion of the normal-force coefficient (linear or nonlinear) that is independent of σ has been handled as described in the previous section concerning axisymmetric bodies. Portions of the normal-force derivatives that are dependent on σ have been assumed to

vary linearly with δ. Hence these components have been handled consistent with the previous section concerning in-plane and out-of-plane force derivatives that are functions of σ. Note that any part of the force derivative that is nonlinear and dependent on σ has been assumed negligibly small. This assumption is believed to be quite valid. It is felt that these approximate expressions for the force variations with σ are reasonable, and attempts to refine them further are not justified until more experimental data for asymmetric bodies become available. Thus,

$$C_{N_z} = \left(C_{N_z}\right)_o + C_{N_\alpha}\left(\frac{w}{V}\right) + \Delta C_{N_\beta}\left[\frac{|v|}{\sqrt{w^2 + v^2}}\right]\frac{w}{V} - 2K_1\left[\frac{v^2 w}{V(w^2 + v^2)}\right] + C_{N_{3\delta}}\left[\left(\frac{w}{V}\right)^3 + \frac{v^2 w}{V^3}\right] \tag{12}$$

and

$$C_{N_y} = \left(C_{N_y}\right)_o + C_{N_\alpha}\left(\frac{v}{V}\right) + \Delta C_{N_\beta}\left[\frac{|v|}{\sqrt{w^2 + v^2}}\right]\frac{v}{V} + 2K_1\left[\frac{w^2 v}{V(w^2 + v^2)}\right] + C_{N_{3\delta}}\left[\left(\frac{v}{V}\right)^3 + \frac{w^2 v}{V^3}\right] \tag{13}$$

The corresponding moment expressions including terms resulting from the above in-plane and out-of-plane forces can be written:

$$C_n = C_{n_o} - C_{m_\alpha}\left(\frac{v}{V}\right) + \Delta C_{n_\beta}\left[\frac{|v|}{\sqrt{w^2 + v^2}}\right]\frac{v}{V} + 2K_2\left[\frac{v w^2}{V(w^2 + v^2)}\right] - C_{m_{3\delta}}\left[\left(\frac{v}{V}\right)^3 + \frac{v w^2}{V^3}\right] \tag{14}$$

and

$$C_m = C_{m_o} + C_{m_\alpha}\left(\frac{w}{V}\right) - \Delta C_{n_\beta}\left[\frac{|v|}{\sqrt{w^2 + v^2}}\right]\frac{w}{V} + 2K_2\left[\frac{v^2 w}{V(w^2 + v^2)}\right] + C_{m_{3\delta}}\left[\left(\frac{w}{V}\right)^3 + \frac{v^2 w}{V^3}\right] \tag{15}$$

Finally, for missile-type vehicles which usually experience small roll rates, the σ-dependent increment to the roll moment can have, in some cases, the most significant σ-dependent effect on the motion of the body. The assumed variation of this increment with σ is

$$\Delta C_\ell = \sin\left(N\sigma\right)\left(C_{\ell_{\sigma_1}} \sin\delta + C_{\ell_{\sigma_2}} \sin^2\delta\right)$$

This variation follows from the boundary conditions (see Sketch 1), $\Delta C_\ell = 0$ for $\sigma = 0$ and 90 deg. Hence, for the present elliptic bodies, N = 2, and the rolling-moment coefficient as used in this report can be written:

$$C_\ell = C_{\ell_p}\left(\frac{pd}{2V}\right) + \sin(N\sigma)\left[C_{\ell_{\sigma_1}}\left(\frac{\sqrt{w^2+v^2}}{V}\right) + C_{\ell_{\sigma_2}}\left(\frac{w^2+v^2}{V^2}\right)\right] \tag{16}$$

By using the above listed expressions for inertia terms and static aerodynamic force and moments and also accounting for the gravitational force and damping moments, the basic motion equations as revised for asymmetric bodies can be written, viz.,

$$\dot{p} = \{+pq\,I_{xz}(I_x + I_z - I_y) + qr[-I_{xz}^2 + I_z(I_y - I_z)] + I_{xz}qAd\,C_n + I_z qAd\,C_\ell\}\frac{1}{I_x I_z - I_{xz}^2} \tag{17}$$

$$\dot{q} = [+pr(I_z - I_x) + I_{xz}(r^2 - p^2) + qAd\,C_m]\frac{1}{I_y} \tag{18}$$

$$\dot{r} = \{+qr\,I_{xz}(I_y - I_x - I_z) + pq[I_{xz}^2 + I_x(I_x - I_y)] + I_{xz}qAd\,C_\ell + I_x qAd\,C_n\}\frac{1}{I_z I_x - I_{xz}^2} \tag{19}$$

$$\dot{u}_o = -\left(\frac{\rho A}{2m}\right)V^2[+C_x\cos\theta\cos\psi + C_{N_y}(\sin\theta\cos\psi\sin\phi - \sin\psi\cos\phi) + C_{N_z}(\sin\theta\cos\psi\cos\phi + \sin\psi\sin\phi)]$$

$$\dot{v}_o = -\frac{\rho A}{2m}V^2[C_x\cos\theta\sin\psi + C_{N_y}(\sin\theta\sin\psi\sin\phi + \cos\psi\cos\phi) + C_{N_z}(\sin\theta\sin\psi\cos\phi - \cos\psi\sin\phi)]$$

$$\dot{w}_o = -\frac{\rho A}{2m}V^2[-C_x\sin\theta + C_{N_y}\times\sin\phi\cos\theta + C_{N_z}\cos\phi\cos\theta] + g$$

where,

$$C_\ell = C_{\ell_o} + C_{\ell_p}\left(\frac{pd}{2V}\right) + \sin(N\sigma)\left[C_{\ell_{\sigma_1}}\left(\frac{\sqrt{w^2+v^2}}{V}\right) + C_{\ell_{\sigma_2}}\left(\frac{w^2+v^2}{V^2}\right)\right]$$

$$C_m = (C_{m_o}) + C_{m_\alpha}\left(\frac{w}{V}\right) - \Delta C_{n_\beta}\left(\frac{|v|}{\sqrt{w^2+v^2}}\right)\frac{w}{V}$$

$$+ 2K_2\left(\frac{v^2 w}{V(w^2+v^2)}\right) + C_{m_{3\delta}}\left(\left(\frac{w}{V}\right)^3 + \frac{v^2 w}{V^3}\right) + \overline{C_{m_q}}\left(\frac{qd}{2V}\right)$$

$$C_n = (C_{n_o}) - C_{m_\alpha}\left(\frac{v}{V}\right) + \Delta C_{n_\beta}\left(\frac{|v|}{\sqrt{w^2+v^2}}\right)\frac{v}{V}$$

$$+ 2K_2\left(\frac{vw^2}{V(w^2+v^2)}\right) - C_{m_{3\delta}}\left(\left(\frac{v}{V}\right)^3 + \frac{vw^2}{V^3}\right) + \overline{C_{m_q}}\left(\frac{rd}{2V}\right)$$

$$C_x = C_{x_o} + C_{x_\alpha}\left(\frac{w^2+v^2}{V^2}\right) + \Delta C_{x_\beta}\left(\frac{|v|\sqrt{w^2+v^2}}{V^2}\right)$$

$$C_{N_y} = (C_{N_y})_o + C_{N_\alpha}\left(\frac{v}{V}\right) + \Delta C_{N_\beta}\left(\frac{|v|}{\sqrt{w^2+v^2}}\right)\frac{v}{V}$$

$$+ 2K_1\frac{w^2 v}{V(w^2+v^2)} + C_{N_{3\delta}}\left(\left(\frac{v}{V}\right)^3 + \frac{w^2 v}{V^3}\right)$$

$$C_{N_z} = (C_{N_z})_o + C_{N_\alpha}\left(\frac{w}{V}\right) + \Delta C_{N_\beta}\left(\frac{|v|}{\sqrt{w^2+v^2}}\right)\frac{w}{V}$$

$$- 2K_1\left(\frac{v^2 w}{V(w^2+v^2)}\right) + C_{N_{3\delta}}\left(\left(\frac{w}{V}\right)^3 + \frac{v^2 w}{V^3}\right)$$

Note that the above angular motion equations define the motion relative to the fixed-body axes, whereas the translational motion equations define that motion relative to earth-fixed axes.

The programming required to incorporate the motion equations for asymmetric bodies into the NIF technique was accomplished on contract

with Armament Systems Department, General Electric Company, Burlington, Vermont. Programming aspects of the NIF technique are discussed in detail by Whyte and Hatheway of the General Electric Company in Ref. 4. The fitting programs are of an iterative type in which adjustments to the equation parameters being determined are obtained using the method of least squares and differential corrections. These programs have considerable flexibility in that the individual aerodynamic parameters listed in the above equations may be fitted or held constant. Further, the programs include additional aerodynamic terms, not listed, which permit handling motion histories for bodies having higher-order nonlinearities or for the more simple bodies having aerodynamic and inertia symmetry.

Some of the roll-dependent aerodynamic terms listed in the above equations reflect modifications to terms initially included in the present programs. These modifications are currently being incorporated into the programs.

3.0 APPARATUS

3.1 RANGE

Range G consists of a 10-ft-diam, 1000-ft-long tank that is contained within an underground enclosure (see Fig. 2). It is a variable-density aerodynamic range and contains 53 dual-plane shadowgraph stations. Forty-three of the stations are positioned at nominal 20-ft intervals, yielding an 840-ft instrumented length. The spacing of the other stations is such that a station is located approximately 10 ft downrange of stations 5 through 10, 12, 13, 15, and 16. The angular orientation and position of most test configurations can be determined to within approximately ±0.25 deg and ±0.002 ft, respectively, at each station. A chronograph system measures intervals of flight time to within $\pm 2 \times 10^{-7}$ sec. The range pumping system provides range pressures from 1.7 atm down to about 20 μHg. The nominal operating temperature of the range is 76°F. The launcher used in this investigation is a two-stage, light-gas gun having a 2.5-in.-diam launch tube.

3.2 CONES AND TEST CONDITIONS

Four elliptic cones of the same configuration were flight tested. A configuration sketch is shown in Fig. 3. The cones had a minor-to-major axis ratio of 0.75 and were constructed of aluminum with a Fansteel® 60 nose tip. Two pins (0.025- and 0.04-in.-diam) were

inserted into the base of each cone. These pins protruded from the base 0.1 in. and provided a means for obtaining the roll orientation of the cone as a function of flight time.

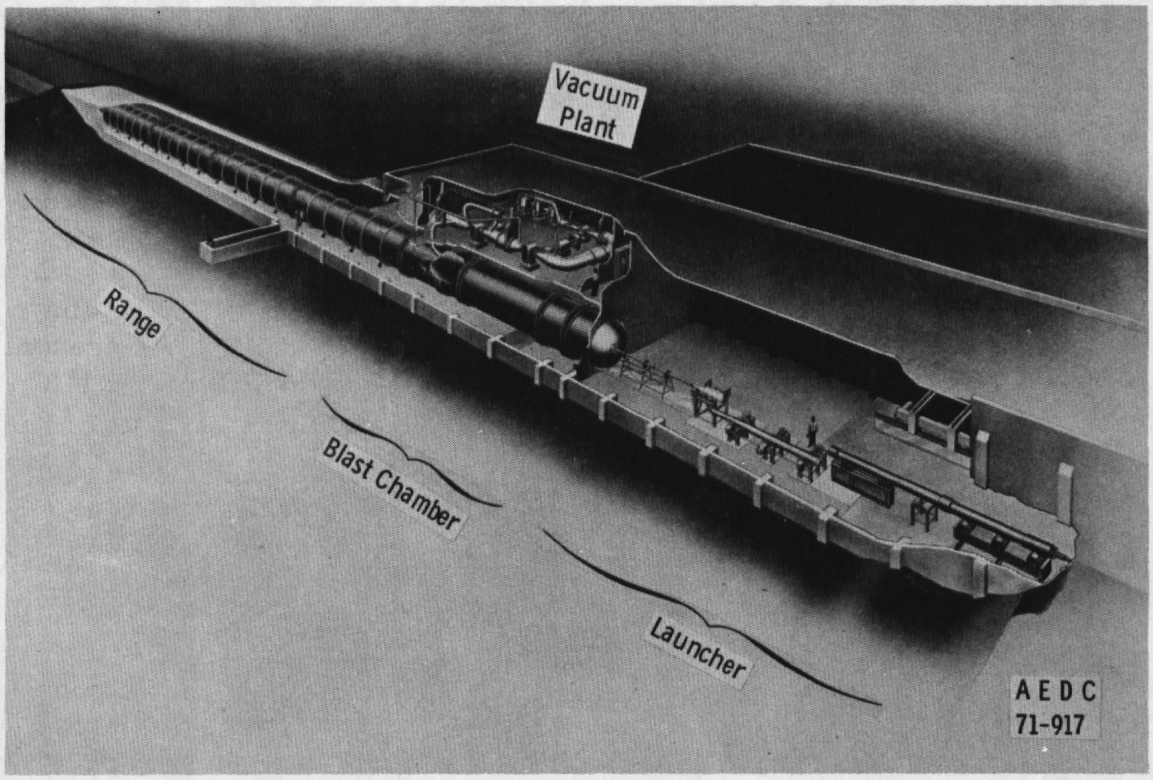

Figure 2. Range G.

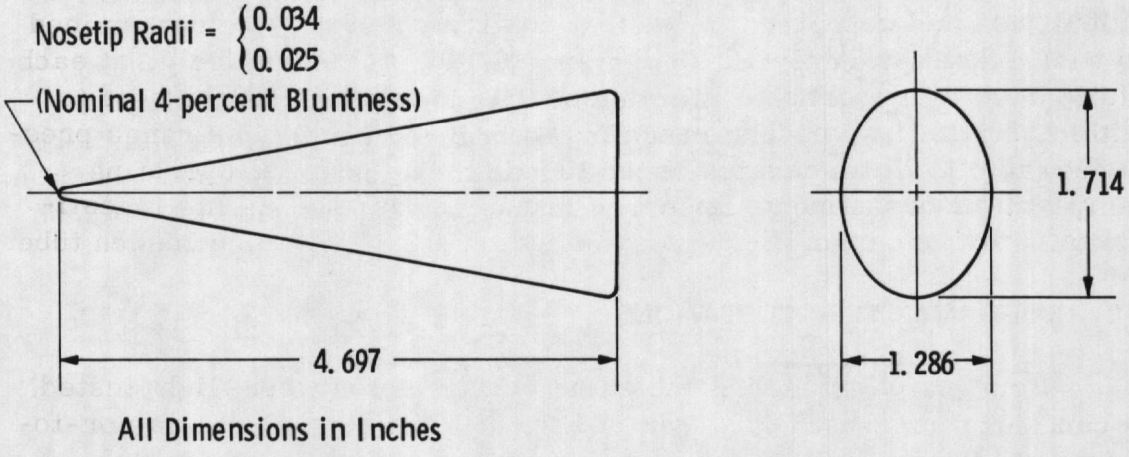

Figure 3. Elliptic cone.

A typical four-component sabot was utilized in launching the cones. The sabots were constructed of Lexan®, and all cones were launched in an uncanted orientation relative to the sabot. The initial angular disturbances to the cones were those arising from muzzle effects and from the cone-sabot separation process.

The four cones were tested at a Mach number of about 7.5 and a Reynolds number, based on cone length and free-stream conditions of about 2.7×10^6. The physical characteristics and test conditions of the individual cones are listed in Table 1.

Table 1. Test Conditions and Physical Characteristics of the Elliptic Cones Investigated

Shot No.	M	$Re_\ell \times 10^{-6}$	m, gm	$I_x \times 10^4$, in.-lb-sec^2	$I_y \times 10^4$, in.-lb-sec^2	$I_z \times 10^4$, in.-lb-sec^2	ψ^a	
							α-plane	β-plane
1	7.3	2.6	105.38	1.08	9.11	8.79	0.026	0.033
2	7.4	2.6	106.07	1.09	9.23	8.89	0.028	0.036
3	7.7	2.8	99.95	1.09	9.32	8.97	0.033	0.039
4	7.6	2.7	99.30	1.07	9.29	8.95	0.035	0.047

[a]Nose Bluntness Ratio

4.0 UNCERTAINTIES IN AERODYNAMIC PARAMETERS

It is significant to note that the experimental errors of concern in ballistic range aerodynamic measurements are, in general, of a random nature. Therefore, it is felt that the spread in the measurements of an aerodynamic parameter provide the best estimate of the total uncertainty in that parameter.

Although experience in reducing data using the current fitting programs are limited, uncertainties in the reduced parameters should be comparable to the estimates listed below; these estimates are based on spreads in measurements observed in the present test and in previous Range G test programs.

Coefficient	C_D	C_M	C_N	cp	$\overline{C_{m_q}}$
Estimated Total Uncertainty (2σ)*, %	1.5	2	5	0.3	10

*σ-Standard deviation of measurements

5.0 DISCUSSION

Representative plots of the yawing and rolling motions of the elliptic cone shots are shown in Fig. 4. The reversal in the rolling motion (ϕ) is of particular interest because such a reversal is normally not experienced by an axisymmetric body. Satisfactory fits were obtained for the motions of the four cone shots although residuals of fit were, in general, about 25 percent higher than residuals normally observed in motion fits of axisymmetric bodies. Accounting for the roll moment contribution that is σ-dependent was shown to be very important as the inclusion of the $C_{\ell_{\sigma 1}}$ term was necessary to permit satisfactory fits of the motions of these shots. However, only linear aerodynamic force and yawing moments asymmetries were used (C_{N_α} and C_{N_β}, and C_{m_α} and C_{m_β}). It is felt that any nonlinearities associated with the small nose bluntness ratios of the present tests would be negligibly small; however, the σ-dependent force and moment terms discussed previously and currently being incorporated into the fitting programs would be expected to permit some improvement in the motion fits. It is important to note that attempts to fit the measured

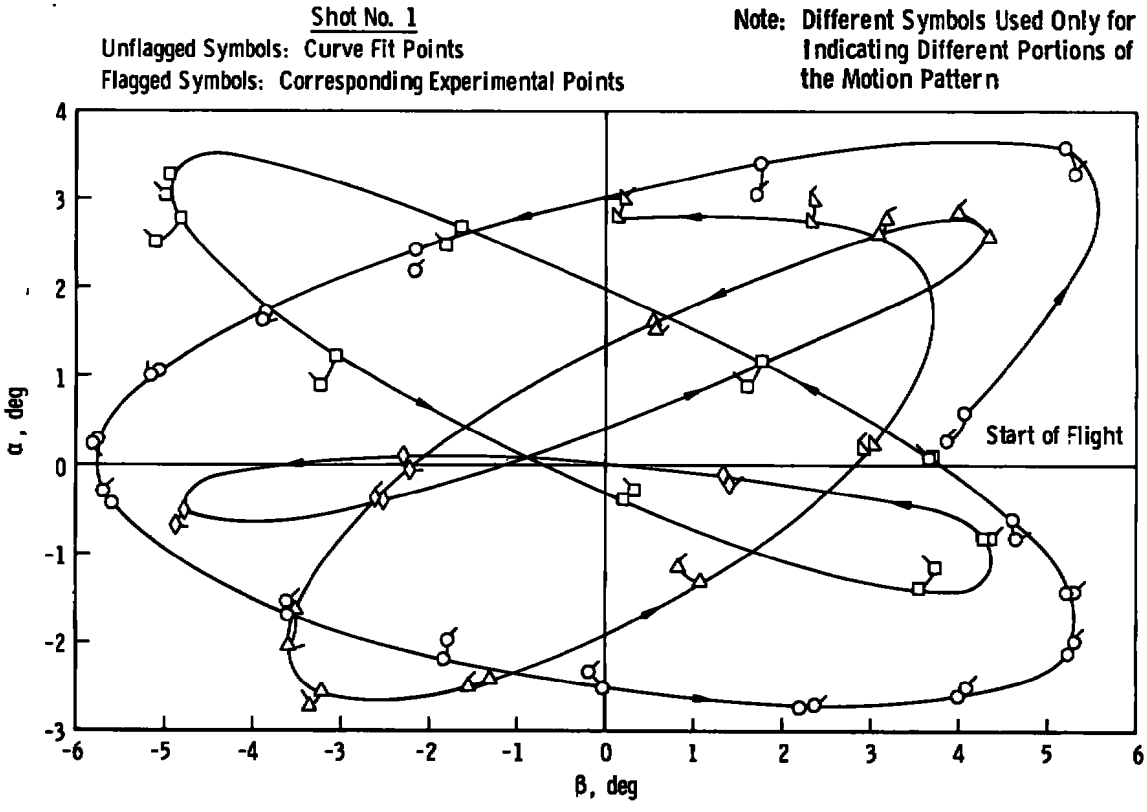

a. Yawing motion

Figure 4. Representative motion patterns for the elliptic cones.

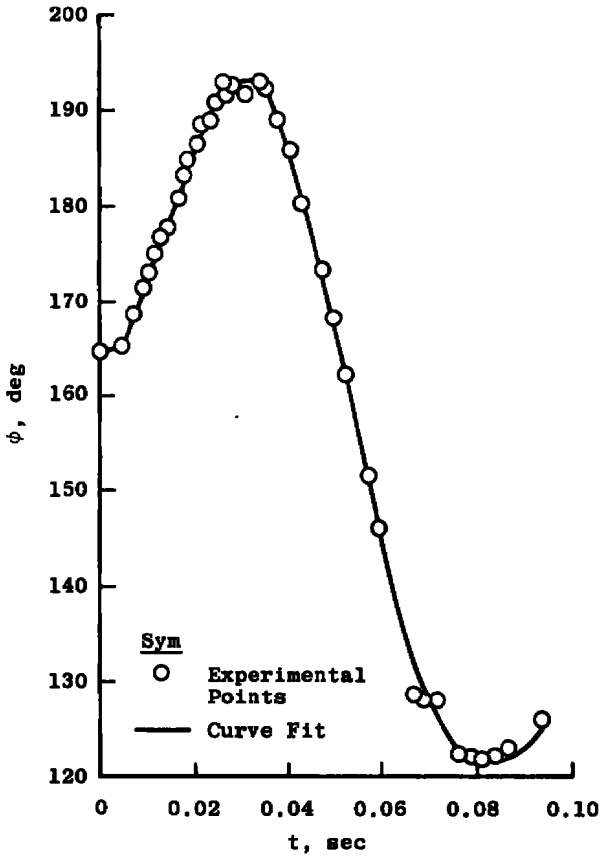

b. Rolling motion
Figure 4. Concluded.

motion histories of the elliptic cones using the previously developed fitting programs designed for axisymmetric bodies failed completely.

The aerodynamic data obtained for the elliptic cones are presented in Figs. 5 through 10. In Fig. 5, the components of the normal force coefficient are shown as functions of the amplitude experienced in the pitch and yaw planes. The force measurements in each plane are consistent for the four shots. For the cone roll orientation indicated in Fig. 5 (major axis of the elliptic cross section in the α-plane), the measurements indicate that the force derivative in the α-plane is approximately 70 percent of that measured in the β-plane, which is indicative of an appreciable configuration asymmetry. Motion fitting attempts involving nonlinear force terms did not produce any detectable improvements in the quality of fits. A comparison of the present normal force data, as a function of ellipticity, with Newtonian predictions from Ref. 7 is shown in Fig. 6 and indicates good agreement between the predicted and experimental values.

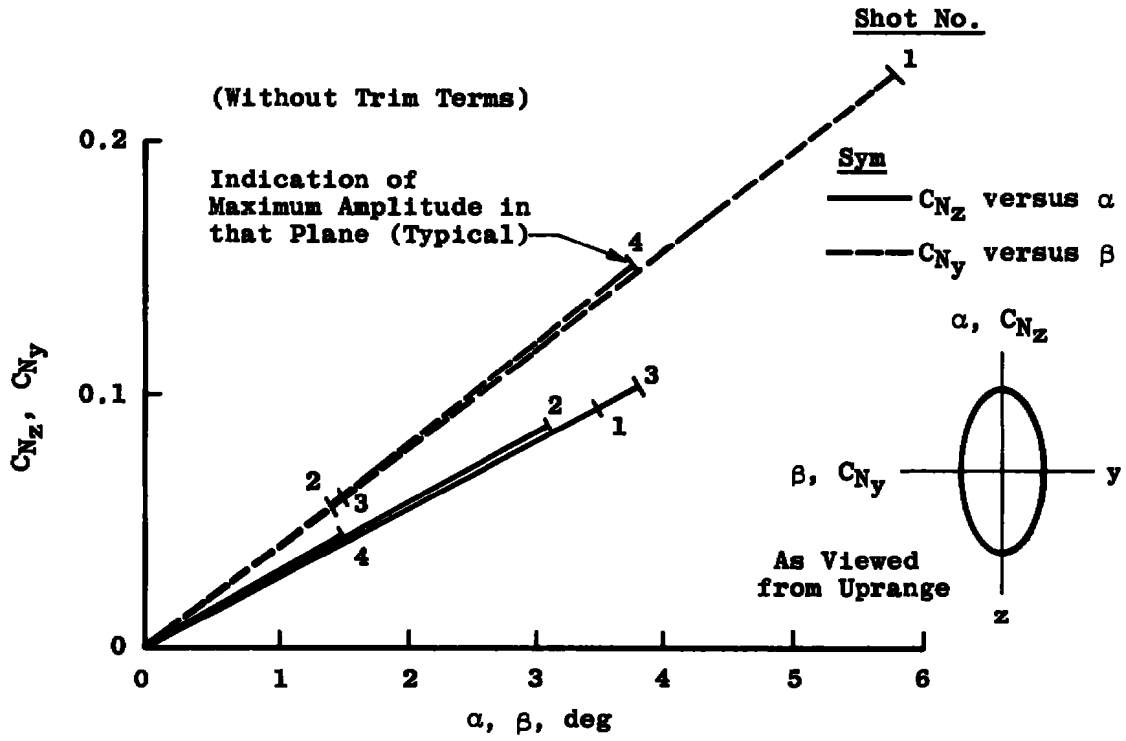

Figure 5. Normal force coefficients.

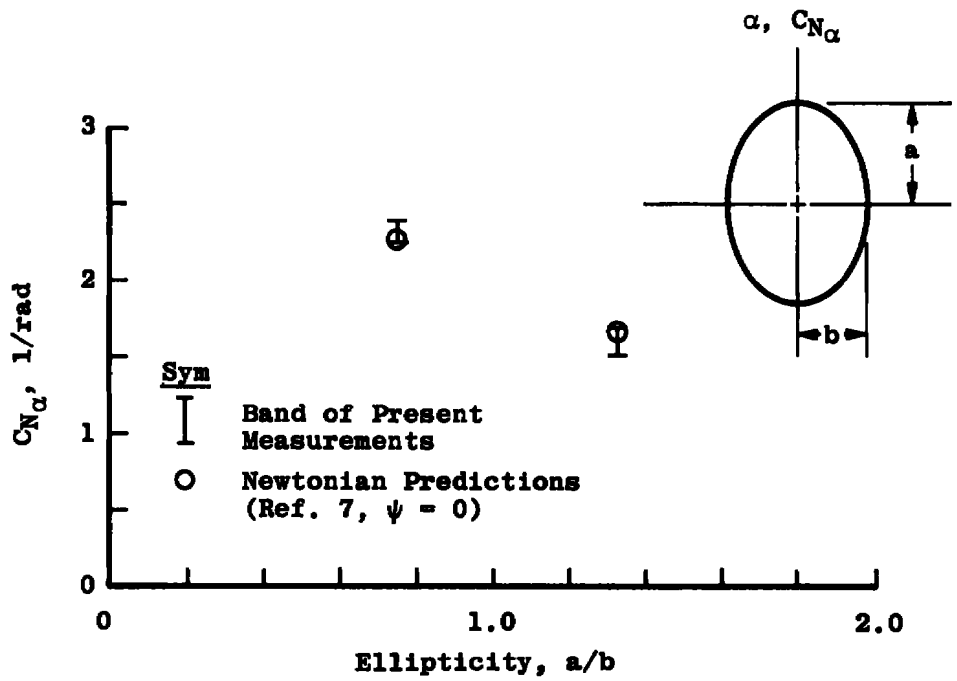

Figure 6. Comparison of experimental and predicted force derivatives.

The moment data are presented in Fig. 7 and indicate similar effects of the configuration asymmetry as observed in the force data. Apparent deviations in the measurements for shots 3 and 4, and for shots 1 and 2, in the α-plane, are believed associated with differences in nose bluntness ratio, (ψ) (see Table 1). In Fig. 8, the center of pressure (cp) data are shown as a function of the nose bluntness ratio. Though the measurements do not indicate a detectable difference in cp between the two planes, they do suggest a bluntness effect. A similar effect of ψ on cp has been observed previously for axisymmetric bodies (see for example, Ref. 8). Note that the observed differences in nose bluntness resulted from construction deviations and were not intentional.

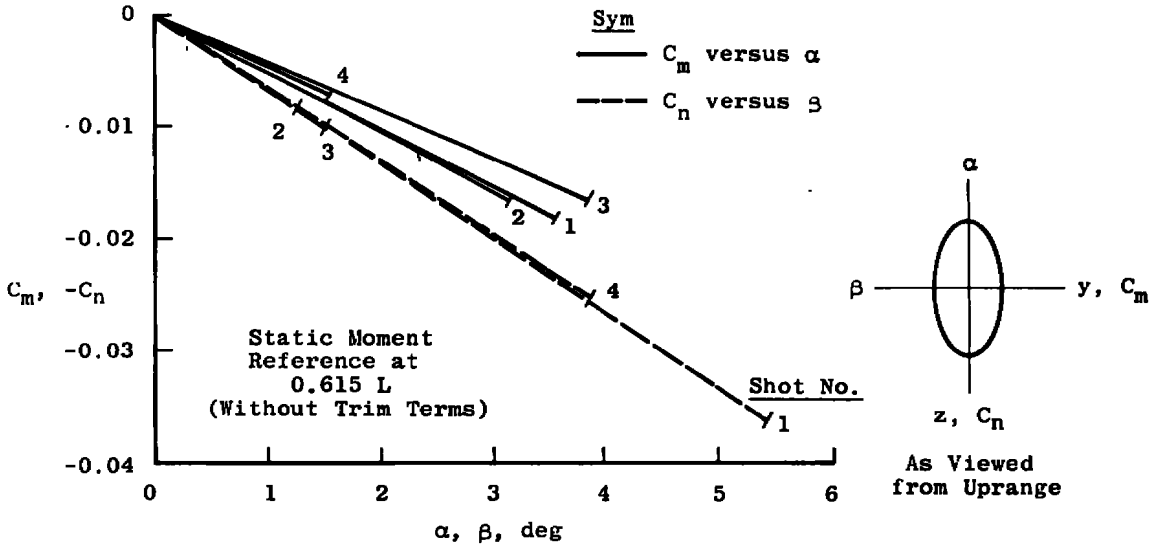

Figure 7. Moment coefficients.

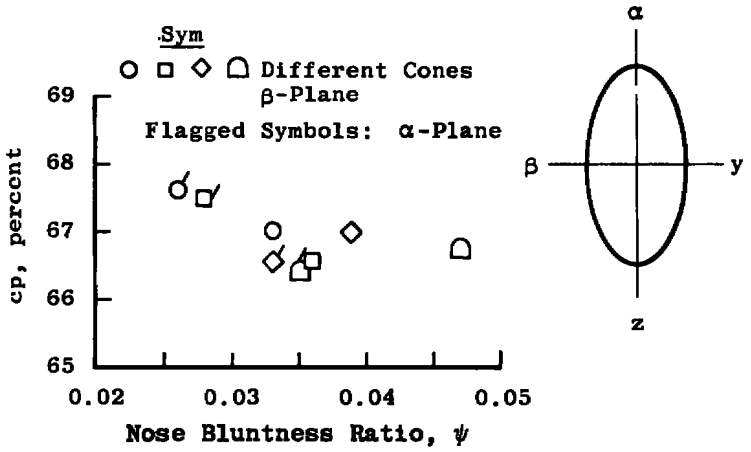

Figure 8. Variation of center of pressure with bluntness.

The mean damping derivative ($\overline{C_{m_q}}$) is shown in Fig. 9. No measurable asymmetry in the damping moments between the pitch and yaw planes was detected. The scatter in the measurements is believed related to the small amplitude levels of the present shots.

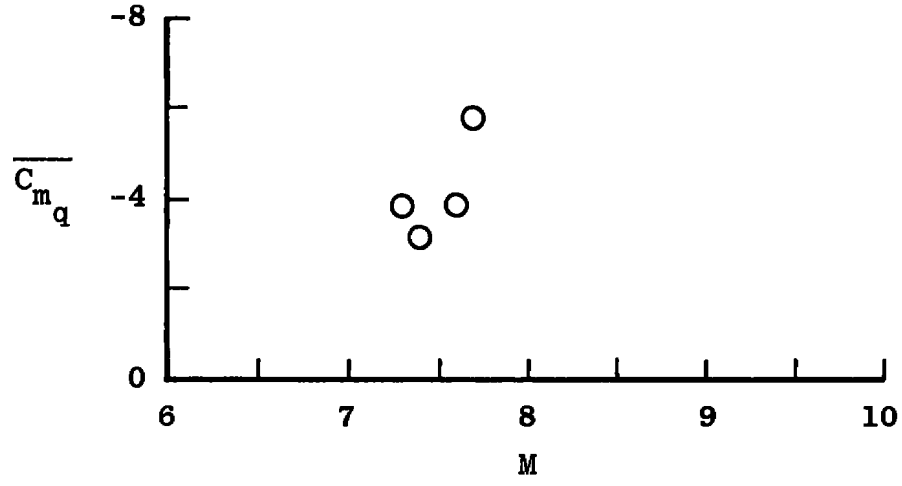

Figure 9. Damping derivative.

The mean drag coefficient ($\overline{C_D}$) is shown in Fig. 10 as a function of the mean amplitude experienced in the flights. Attempts to detect differences in the drag coefficient for the α- and β-planes were unsuccessful.

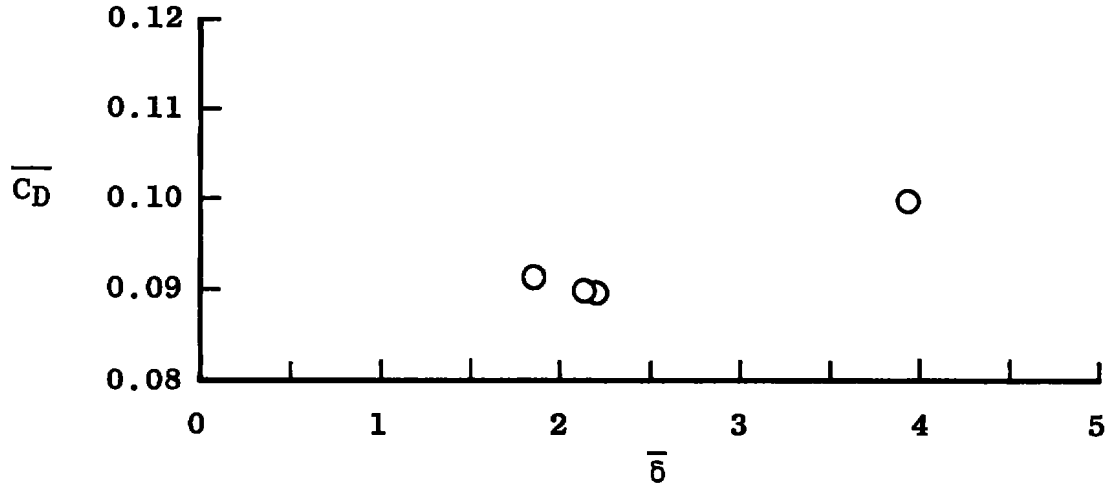

Figure 10. Mean drag coefficient.

The experimental data presented are significant in that they are believed to be the first free-flight data obtained for such bodies and they indicate that the present motion analysis procedure provides a useful extension to the free-flight testing capability. It should be noted that one can expect asymmetries in the drag and damping moment always to be difficult to detect at small amplitudes. This follows because the effects of these two parameters on motion histories are small when small amplitudes are involved.

A logical extension to the present effort would be further revisions in the aerodynamic expressions to account for magnitude changes in a derivative, such as $C_{m_{\dot{\alpha}}}$, as the angular motion changes sign. Such extensions are obviously desirable as they would permit handling asymmetries of greater complexity.

The elliptic configuration of the present test has two planes of symmetry, and hence no cross product of inertia terms were involved. However, a more general asymmetric configuration has only one plane of symmetry, and consistent with the equations of this report, I_{xz} can have a non-zero value. As I_{xz} can be difficult to define experimentally, it represents an area of concern in testing general asymmetric configurations. It was initially believed that there was a possibility that I_{xz} could be treated as one of the unknowns in the motion fitting procedure and it could be determined similarly to the unknown aerodynamic parameters. Hence, in the present programs, the motion equations were programmed to permit an option of treating I_{xz} as either a known or an unknown. A limited study using generated motions (with and without simulated experimental errors in the model orientation angles and displacements) has indicated that I_{xz} can be determined satisfactorily in the fitting procedure. To date simulated vehicles with an inertia ratio (I_{xz}/I_y) up to 0.06 have been examined, and the aerodynamic parameters were evaluated quite well when I_{xz} was treated as an unknown in the motion fits. It is important to note that for the higher end of the (I_{xz}/I_y) ratio band examined, the aerodynamic parameters could not be determined if I_{xz} was ignored in fitting the motion, that is, assumed to be zero. Confirmation that I_{xz} can, in general, be handled as above requires examination of a wide range of motion patterns.

6.0 CONCLUDING REMARKS

A numerical-integration, motion-fitting procedure previously developed for axisymmetric bodies has been extented to vehicles having

appreciable aerodynamic and inertia asymmetries. The primary problem in the extension of the procedure is related to the required revisions to the expressions defining the aerodynamic forces and moments which, for asymmetric bodies, can be very dependent on the roll orientation of the body relative to the plane of the total yaw angle.

Experimental free-flight data are presented for a cone of elliptic cross section that has appreciable aerodynamic asymmetries. These data indicate the potential usefulness of the developed motion analysis procedure.

REFERENCES

1. Dayman, Bain, Jr. "Free-Flight Testing in High-Speed Wind Tunnels." AGARDograph 113, May 1966.
2. Welsh, C. J., Winchenbach, G. L., and Madagan, A. N. "Free-Flight Investigation of the Aerodynamic Characteristics of a Cone at High Mach Numbers." AIAA Journal, Vol. 8, No. 2, February 1970.
3. Chapman, C. T. and Kirk, Donn B. "A Method for Extracting Aerodynamic Coefficients from Free-Flight Data." AIAA Journal, Vol. 8, No. 4, April 1970.
4. Whyte, Robert H. and Hathaway, Wayne H. "Aeroballistic Range Data Reduction Technique Utilizing Numerical Integration." AFATL-TR-74-41, February 1974.
5. Murphy, Charles, H. "Free-Flight Motion of Symmetric Missiles." BRL Report No. 1216, July 1963.
6. Etkin, Bernard. "Dynamics of Flight," John Wiley and Sons, Inc., New York, London, Sydney, Sixth Printing, May 1967.
7. Graham, Ralph E., Lamb, Robert H., and Romere, Paul O. "Newtonian Aerodynamic Characteristics of Blunted Right Elliptical Cones for Cone Thickness Ratios of 0.25 to 3." NASA-TN-D-3462, August 1966.
8. Jones, Jerry H. "Force Tests on 9- and 6.3-deg Half-Angle Cones with Various Simulated Damaged Noses at Mach Number 12." AEDC-TR-70-29 (AD866327), March 1970.

NOMENCLATURE

A	Reference area (cone base area)
$\overline{C_D}$	Mean drag coefficient for flight
C_ℓ	Rolling-moment coefficient
C_{ℓ_σ}	σ-dependent rolling moment derivative
C_m	Moment coefficient (α-plane)
$\overline{C_{m_q}}$	Mean damping derivative for flight, $\left[\frac{\partial C_m}{\partial q(d/2v)} + \frac{\partial C_m}{\partial \dot{\alpha}(d/2v)}\right]$
C_{m_α}, $C_{m_{3\alpha}}$	Linear and nonlinear moment coefficients (α-plane)
C_{m_δ}, $C_{m_{3\delta}}$	Linear and nonlinear moment coefficients (δ-plane)
C_{N_z}	Normal-force coefficient (α-plane)
C_{N_y}	Normal-force coefficient (β-plane)
C_{N_α}, $C_{N_{3\alpha}}$	Linear and nonlinear force coefficients (α-plane)
C_{N_β}, $C_{N_{3\beta}}$	Linear and nonlinear force coefficients (β-plane)
C_{N_δ}, $C_{N_{3\delta}}$	Linear and nonlinear force coefficients (δ-plane)
C_n	Moment coefficient (β-plane)
C_{n_β}, $C_{n_{3\beta}}$	Linear and nonlinear moment coefficients (β-plane)
cp	Center of pressure (percent of cone length)
d	Moment reference length (cone base diameter)
H	Angular momentum of the cone
I_x, I_y, I_z	Moments of inertia
I_{xz}, I_{xy}, I_{yz}	Products of inertia
L	Linear momentum of the cone

M	Mach number
m	Mass of the cone
Re_ℓ	Reynolds number based on free-stream conditions and cone length
p, q, r	Angular velocity components of the fixed-body axis system
u, v, w	Linear velocity components of the fixed-body axis system
x, y, z	Fixed-body axis system (see Fig. 1)
x_o, y_o, z_o	Earth-fixed axis system (see Fig. 1)
V	Velocity of cone
α	Components of total angle of attack in the pitch plane
β	Components of total angle of attack in the yaw plane
δ	Total angle of attack
σ	Roll orientation angle of the plane of the total yaw angle relative to the fixed-body axis system (see Sketch 1)
ψ, θ, ϕ	Euler angles, ψ is also nose bluntness ratio (nose radius/base radius)

SUBSCRIPTS

x, y, z	Indicate directions along fixed-body axes
0	Indicates coefficient at zero yaw angle

SUPERSCRIPT

	Derivative with respect to time